Diplomarbeit

Overview of the animal models of right ventricular dysfunction

eingereicht von

Bakytbek Egemnazarov

zur Erlangung des akademischen Grades

Doktor der gesamten Heilkunde

(Dr. med. univ.)

an der

Medizinischen Universität Graz

ausgeführt am

Lehrstuhl für Physiologie

unter der Anleitung von

PD Dr. Grazyna Kwapiszewska-Marsh

Dr. Leigh Marsh

Graz, am 21.01.2019.

Eidesstattliche Erklärung

Ich erkläre ehrenwörtlich, dass ich die vorliegende Arbeit selbstständig und ohne fremde Hilfe verfasst habe, andere als die angegebenen Quellen nicht verwendet habe und die den benutzten Quellen wörtlich oder inhaltlich entnommenen Stellen als solche kenntlich gemacht habe.

Graz, am 21.01.2019. *Bakytbek Egemnazarov eh.*

Zusammenfassung

Funktion des rechten Ventrikels (RV) bestimmt die schwere der Krankheit und Überlebensdauer von PatientInnen, die an Lungenhochdruck leiden. Chronische RV Drucküberlast führt zur Entwicklung von Dysfunktion des rechten Ventrikels, was später als Rechtsherzversagen endet. Die Mechanismen, die zur RVD Entwicklung führen, sind zum großen Teil unerforscht. Eins von den mehreren Gründen dafür könnte die Tatsache sein, dass heutzutage verwendete Tiermodelle wiederspiegeln den komplexen RV Dysfunktion Syndrom nicht komplett und dadurch nicht zufriedenstellend sind. Ziel dieser Arbeit bestand darin durch eine Literaturrecherche die Eigenschaften der RV Dysfunktion, die durch existierende Tiermodelle nicht nachgeahmt werden, zu entdecken. Darüber hinaus, die Aspekte der RV Pathophysiologie, die zur Zeit wenig erforscht werden, sollen identifizieren werden. Die gewonnenen Kenntnisse sollten uns die Ideen zur Verbesserung unserer Modelle liefern.

Im Rahmen dieser Arbeit wurde eine Literaturrecherche durchgeführt. Ergebnisse unserer Gruppe wurden mit den Daten von anderen Gruppen verglichen.

Zurzeit, Untersuchungen von RV Dysfunktion befinden sich auf dem Niveau der Charakterisierung. Hypoxia induzierte RVD Modell scheint ein Modell der komplett kompensierter Drucküberlast zu sein. Pulmonary artery banding (PAB) Modell löst eine ausgeprägte adaptive RV Umbau aus, was funktionell moderate Dysfunktion verursacht. Monocrotalin (MCT) und Sugen5416 (SU/HOX) induzierte Modelle verursachen stärkere Dysfunktion. Dabei keine der Modelle zeigt den Phänotyp der Herzdekompensation. Molekularbiologische Untersuchungen zeigen Beteiligung von verschiedenen Signaltransduktionswege, die teilweise durch die Untersuchungen von linksventrikulärer Dysfunktion bekannt sind. Charakterisierung mittels invasiver und nicht-invasiver Techniken zeigt verminderte Herzfunktion in PAB, MCT und SU/HOC Modellen. Dabei die Frage der Kopplung von RV und der Pulmonalarterie (RV/PA coupling) bleibt meistens nicht untersucht. Zusammengefasst. Klinisches Bild des Rechtsherzversagens wird in keiner untersuchten Modells nachgeahnt. Molekulare Mechanismen der RV Dysfunktion und Versagens scheinen teilweise spezifisch für RV zu sein. Einige Fragen der RV Physiologie, wie zum Beispiel RV/PA Kopplung, bleiben meistens nicht untersucht.

Abstract

The function of the right ventricle (RV) determines the severity of the disease and survival of patients suffering from pulmonary hypertension. Chronic RV pressure overload leads to development of RV dysfunction, which culminates in heart failure. Mechanisms responsible for development of RV dysfunction are poorly investigated. One of the reasons could be the fact that the currently used animal models do not resemble the complexity of RV dysfunction in full and therefore are not satisfactory. The aim of the work is by performing a literature search elucidate some features of RV dysfunction, which are not reflected by existing animal models. Moreover, some aspects of RV pathophysiology, which are less investigated, should be identified. The obtained knowledge should deliver ideas for improvement of our models.

The literature search was performed for this work. Results of our group were compared with findings of other groups.

Currently, investigations on RV dysfunction are at the level of characterizeing it. Hypoxia induced RV dysfunction model appears as a model with fully compensated pressure overload. Pulmonary artery banding model (PAB) induces pronounced adaptive RV remodeling, which causes moderate dysfunction. Monocrotalin (MCT) and Sugen5416 (SU/HOX) induced models cause severer dysfunction. Although, none of the models demonstrates the phenotype of cardiac decompensation. Investigations using molecular biology approach show contribution of different signaling pathways partly known from the research on the left ventricular dysfunction. Characterization using invasive and non-invasive techniques demonstrates reduced cardiac function in PAB, MCT and SU/HOX models. At the same time, the aspect of RV/PA coupling remains mainly untouched.

Summary. None of the investigated animal models resembles the clinical picture of cardiac failure. The machanisms of RV dysfunction seem to be partly specific for RV. Some questions of RV physiology, e.g. RV/PA coupling, remain poorly investigated.

Inhalt

1. Introduction

1.1. Role of the right ventricle in pulmonary hypertension

Pulmonary arterial hypertension is a disease condition caused by several different factors and characterized by chronic pressure elevation in the lung vasculature (1). This causes chronic elevated load to the right ventricle (RV). Historically, research in the field of PAH was mainly concentrated on the investigations on the lung vasculature (Fig. 1). Recent findings and analysis of meta-data revealed that RV function determines functional status and survival of patients suffering from (PAH) (1). In another words, not the level lung vascular changes but the RV functional status determines how the patient feels and how long he will survive. This urges necessity to study the mechanisms of RV adaptation to PAH to develop novel medicines targeting RV. Several factors have been suggested as contributing to RV failure such as RV ischemia, inflammation and fibrosis (2). Nevertheless, the underlying mechanisms of RV dysfunction are poorly understood (2).

1.2. Limitations of the human studies of RV.

In our era of evidence-based medicine, therapeutic approaches should base on solid scientific knowledge about the pathomechanisms of RV dysfunction and failure. However, a number of factors obscure the investigation of the RV.

Due to its position and complex shape, not all the techniques developed to study left ventricle (LV) are applicable for RV. For instance, thin walls of RV preclude from performing biopsies. Therefore, we are severely limited in ability to perform histologic examinations on RV of PAH patients. A possibility to overcome this limitation could be to analyze LV samples. However, due to known differences between RV and LV this approach might not work. Due to differences in developmental origin, structure and function, the RV response to pathological stimuli could be different from the LV response, e.g. the ventricles respond differently to adrenergic stimulation (3). This mechanism potentially explains responses of the ventricles to norepinephrine (4). Growth factor response is activated differently in response to volume

overload in both ventricles (5). Thus, knowledge obtained so far on the mechanisms of LV adaptation, dysfunction and failure should be extrapolated to the RV with caution.

PAH is a rare disease with prevalence varying between 3 to 10 per million patients (1). Therefore, physiological investigations require longer timeframes to collect patient cohorts of sufficient statistical power. The pressure to treat patients now motivates to look for other alternatives to speed up our progress in understanding the mechanisms of the disease.

1.3. Advantages of animal models.

Investigations on RV function in patients are challenging partly due to before mentioned anatomical factors but also the lack of material for ex vivo studies. . E.g. biopsy of RV wall is not routinely performed due to the high chance of RV perforation, a dangerous complication of the procedure. Therefore, the option to fill the gap in knowledge is to perform studies on animal models. Animal models do not resemble human diseases in full and have some limitations due to differences genetics, metabolism, and physiology (6). Nevertheless, animal models deliver valuable information about physiology, adaptation mechanisms to noxious stimuli. Genetically modified rodent models deliver a unique opportunity to investigate genetics and molecular mechanisms of human diseases. In PAH research, several models have been developed potentially reflecting different etiologies of this disease (6). Currently, growing appreciation of the importance of RV function for the disease progression resulted in constantly growing number of publications reaching 150 per year (Fig. 1). Nevertheless, this represents only 10 % of all publications in PAH field.

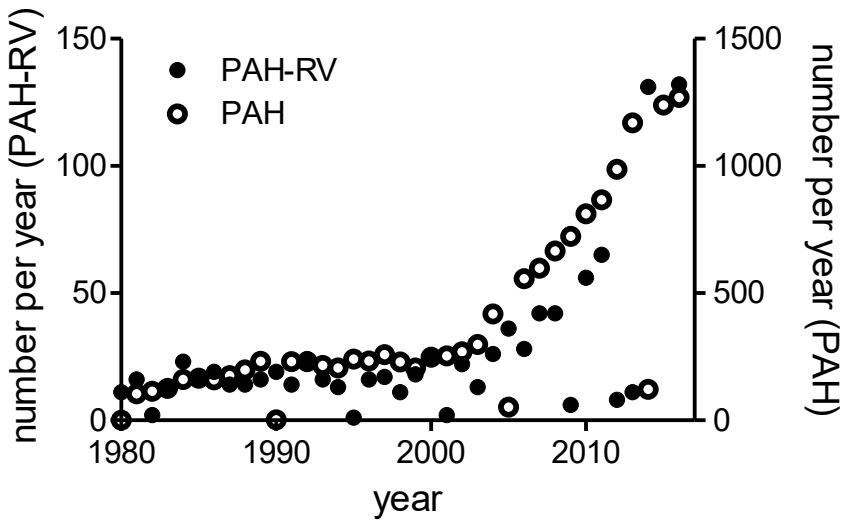

Fig. 1. Dynamic of publications about the right ventricle in the field of PAH. A search was performed in Pubmed using key words “pulmonary arterial hypertension” and the combination of “pulmonary arterial hypertension” and “right ventricle”. The obtained results are analyzed annually and plotted.

1.4. Pathophysiology of pressure overload.

Hemodynamic overload the heart could be of two types: volume overload and pressure overload. Volume overload occurs when RV is filled by too high volume of blood, which happens in the conditions of congenital cardiac defects and disorders of the values. Volume RV overload is out of scope of our study and will not be discussed. Pressure overload is the pathophysiological situation when the heart must contract against elevated resistance (elevated afterload), which occur in the clinical settings of PAH, PA thromboembolism or PA stenosis. Several factors contribute to the RV pressure overload: elevation in vessel resistance, vessel stiffness, disturbance of RV-PA coupling.

1.4.1. Vascular resistance

In the context of cardiovascular physiology, resistance is the load against which the heart should work to eject blood. Since cardiovascular system is a closed circulation consisting of the pump and the vessels, the laws of fluids dynamics are applicable for understanding of its

function. The resistance of the rigid vessels can be calculated using the Hagen–Poiseuille equation:

$$\boldsymbol{R = 8 * L * \eta / (\pi * r^4)}$$

where:

R – resistance to fluid flow

L – length of the vessel

η – viscosity of the fluid

r – radius of the blood vessel

Since in the body the length of the vessels does not change, the factors influencing vessel resistance are blood viscosity and blood vessel radius (diameter). As the vessels radius is to the power of four in the formula, any smallest change in the vessel diameter results in significant increase in resistance. E.g. 15% decrease in radius results in two-fold increase in resistance, 50% radius decrease causes a 16 fold elevation in resistance. However, the lung vascular tree is a complex structure consisting of several segments of vessels with different diameters. Therefore, application of the Hagen–Poiseuille equation for resistance calculation in humans is impossible. Nevertheless, it enables general overview of the factors which are important for the changes in vascular resistance.

For the complex vascular system like pulmonary circulation, another way to measure the resistance is to determine the total vascular resistance using the formula:

$$\boldsymbol{R = \Delta P / Q}$$

where:

ΔP – pressure difference between the beginning and the end of circulation loop corresponding for the small circuit to the pressure in the main pulmonary artery and left atrial pressure.

Q – the flow through the vasculature

In the clinical praxis, the formula is used as follows:

$$\boldsymbol{PVR = (mPAP - PCWP)/CO}$$

where:

PVR – pulmonary vascular resistance

mPAP – mean pulmonary arterial pressure

PCWP – pulmonary capillary wedge pressure, which is taken as a surrogate for the left atrial pressure

CO – cardiac output

This formula is considered to provide the total pulmonary vascular resistance. However, the pressure difference reflects the difference between begin and end of the arterial part of the pulmonary vascular tree. Thus, the formula measures the resistance of the arterial tree and the venous tree is assumed to have a negligible resistance.

The formula has very limited use in small animal research since mPAP is calculated from systolic and diastolic pulmonary arterial pressure (sPAP and dPAP, respectively). Measurement of sPAP and dPAP requires advancement of the pressure sensitve catheter along the pulmonary artery, which is technically very challenging. Therefore, this measurement is rarely used (7). Additional difficulty is measurement of cardiac output in small animals. Due to these technical difficulties, the measurement of the right ventricular systolic pressure (RVSP) has been established as a surrogate of pulmonary vascular resistance. However, very important assumptions are made that cardiac output changes are neglectable and no pressure gradient exists between RV and pulmonary artery.

1.4.2. Vascular stiffness/compliance

The vessels in the body are not rigid but elastic/compliant. The elastic properties of the vessels are responsible for converting pulsatile blood flow ejected by the heart into steady flow in capillaries facilitating diffusion. In the systemic vasculature compliance and resistance are distributed between the large conductance vessels (aorta and large arteries) and small resistance arteries. A specific feature of the lung vasculature is that compliance and resistance

are determined by anatomically closely located vessels and build an inverse relationship (8) (Fig. 2). The normal pulmonary circulation is a low-pressure, high-compliance system. In PAH, pulmonary vascular compliance decreases because of increased extracellular matrix/collagen deposition in the pulmonary arteries. The decreased compliance leads to elevated pulse wave reflection from the stiffened vessels. This in turn increases the pulsatile load on RV. The pulsatile afterload contributes approximately 23% of the workload of RV (9). The vascular compliance has been shown to predict survival of PAH patients (10). Moreover, the vessel stiffness, a parameter inversely related to compliance, has been shown to predict mortality of PAH patients (11).

There are several ways to calculate vascular compliance: Windkessel model (12), pulse pressure method (13), diastolic decay method (14) and area method (12). Due to its technical simplicity, in the clinical practice the pulse pressure method is used more broadly (11):

C=SV/PP

where,

C – compliance

SV – stroke volume

PP – pulse pressure

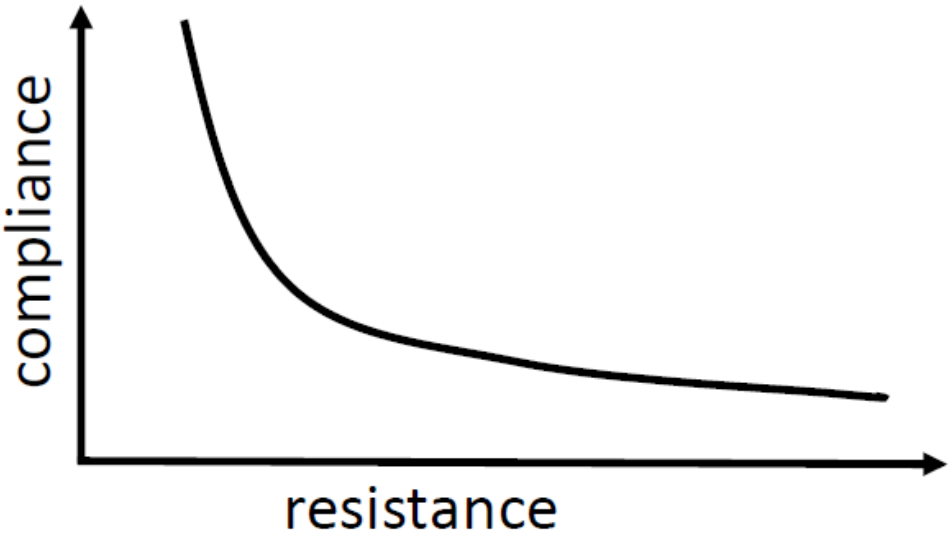

Fig. 2. Relationship between vascular compliance and resistance in pulmonary vasculature. In contrast to systemic vasculature, compliance and resistance in the pulmonary vasculature are determined by anatomically closely located vessels and build an inverse relationship.

1.5. Cardiac function

RV function is determined by properties of the pulmonary vasculature. Under normal conditions, pulmonary vasculature is low resistance and high elastance vessels, which does not require high force development. The filling of the thin walled and right atrium is influenced by respiration being increased during inspiration and decreased during expiration. This causes respiration dependent variation in the filling of RV and requires a compliant chamber, which can provide constant contraction despite variable filling. These two factors determine RV morphology (thin walled and compliant) and function (low pressure pump). RV function is determined by its contractility (systolic function), relaxation (diastolic function) and RV coupling to pulmonary vasculature (RV/PA coupling).

1.5.1. Systolic function.

Systolic function or contractility can be determined as an ability of the heart to generate force sufficient to eject blood into vasculature. Contractility of the heart is dependent on preload

by the Frank-Starling mechanism (15) and afterload by the Anrep mechanism (16). Moreover, cardiac contractility is under control of several neuro-humoral factors (17, 18). Therefore, measurement of RV contractility is difficult. The current gold standard is the determination of the end-systolic elastance (Ees) by varying cardiac load using pressure-volume analysis (19). Mostly, pressure-volume loop analysis is performed using conductance catheters, which has been developed for LV analysis. However, due to differences in shape (crescent RV vs. cylindrical LV), contraction pattern (wave-form and baso-apical movement in RV vs. mainly radial contraction in LV) application of the technique for RV analysis should be undertaken cautiously.

To overcome the limitations of the technique, a single beat method of pressure-volume relationship has been developed (20). The advantage of the proposed method is no need for chamber volume measurements and therefore no manipulation of venous return. However, the method assumes that contractility is the same in the ejecting and isovolumic beats. Therefore, the maximal pressure of the isovolumic beat can be extrapolated from ejecting beat. The method awaits clinical validation studies.

1.5.2. Diastolic function

Diastolic function is determined an ability to relax and accommodate incoming blood volume. Major determinants of diastolic function are active and passive tissue stiffness.

1.5.3. Right Ventricular – Pulmonary Arterial coupling

“Ventriculoarterial coupling” refers to the parameter demonstrating if ventricular contractility increases adequately to load elevation. Mathematically is expressed as a ratio of ventricular contractility to the afterload (21):

Coupling=contractility/afterload

If:

Contractility is determined as a load-independent end-systolic elastance (E_{es}) and afterload is determined as arterial elastance (E_a):

Then

Coupling= Ees/ Ea.

The reference value of the parameter was determined as 1.5-2 (22). This value should be interpreted as a productive mechanical energy transfer from the ventricle to PA after some energy dissipation for heating and friction. The technique based on the cardiac pressure-volume (PV) loop analysis has been developed for the estimation of the LV function and has been transferred for RV functional analysis. Using this estimate the RV of systemic sclerosis patients were found to have more depressed contractile function than RV of PAH patients and RV-pulmonary artery coupling was worse in systemic sclerosis patients (23).

Combination of magnetic resonance imaging (MRI) with simultaneous pressure measurements allows reconstruction of PV loops without any assumptions (24). In the PAH patients, the authors found four-fold elevation in afterload paralleled by two-fold elevation in RV contractility leading to decrease in RV-pulmonary arterial coupling.

1.6. RV adaptation to pressure overload:

1.6.1. Geometry changes, hypertrophy, remodeling

In acute RV response to afterload elevation is the dilation of the ventricle and increase of contractile function via Frank-Starling mechanism (25). In the situation of chronic afterload elevation, like in PAH, increased afterload causes development of the adaptive RV remodeling, which is characterized by RV geometry change to more round shape and hypertrophy (Fig. 3). These changes result in reduction of ventricular wall stress (26). The morphologic substrate of the RV hypertrophy is the increase in cardiomyocyte size through the addition of sarcomeres (27). Consequently, RV contractility increases matching to the elevated load. Excessive pressure overload causes tissue stretching leading to development of RV tissue fibrosis. To some extent RV fibrosis could be a protective mechanism preventing RV from rupture. On the

other hand, excessive RV fibrosis could become pathologic by increasing tissue stiffness (28) or by generating a substrate for arrhythmogenesis (29). An important component of the adaptive remodeling is an adequate increase in RV tissue capillarization (30).

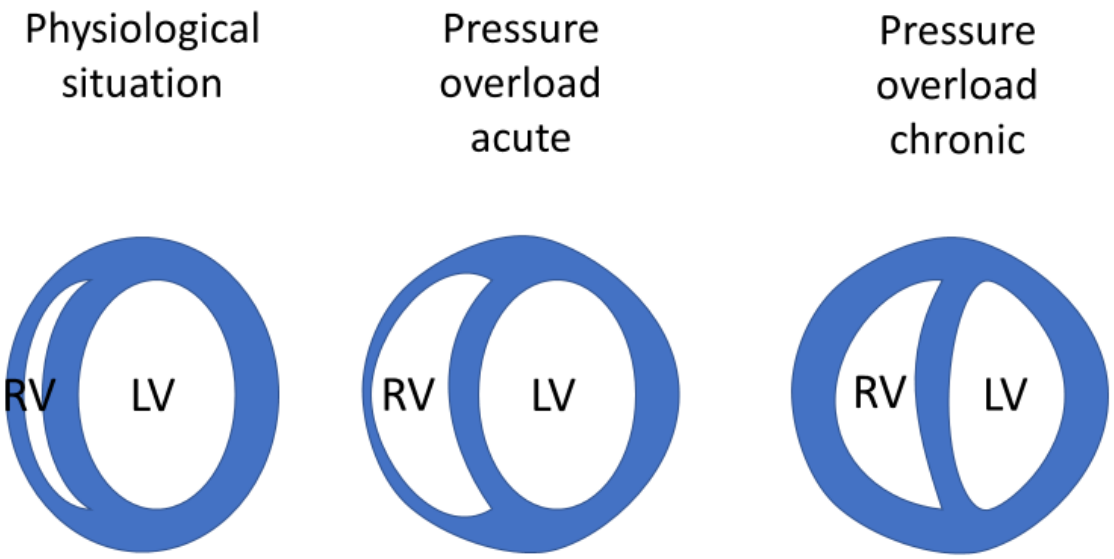

Fig. 3. Acute and chronic right ventricular response to pressure overload. Acute response to the afterload elevation is RV dilation and increase in contractility. Chronic afterload elevation causes RV dilation, hypertrophy and fibrosis.

1.6.2. Transition from adaptation to maladaptation

Despite activation of the above-mentioned mechanisms, at some point RV transits to maladaptation and failure. Mechanisms of the transition are poorly understood.

Several potential scenarios could be supposed:

1. Constantly elevating lung vascular resistance might cause ever growing overload with which RV adaptation mechanisms cannot cope
2. Chronic pressure overload might activate at some point activate some detrimental mechanisms causing maladaptation
3. Adaptation mechanisms under certain conditions could become detrimental per se.

4. Pathological process of the lung vasculature affects RV vasculature causing the disease of the heart and hampering adaptation

A typical example of the scenario 1 is pulmonary embolism. Massive embolism in absence of RV support is a severe clinical situation with high mortality (31). In situations of rapidly progressing PAH, failure of RV to adapt to overload by remodeling can be detrimental (32).

PAH is a progressive disease with ongoing vascular remodeling. Low levels of pressure overload cause RV hypertrophy (33), while higher levels of overload cause additionally fibrosis development (34). Thus, higher levels of pressure overload could potentially activate different molecular pathways some them being maladaptive.

Adaptation mechanisms can be detrimental per se. Activation of the sympathoadrenal system is an adaptive response to the reduced cardiac output. However, chronic overactivation of the system is deleterious causing exhaustion of the cardiac reserve and contributing to mortality (35). Investigations of other adaptation mechanisms should reveal the limits of their protective action.

Dysregulation of the vascular tone is a key feature of the PAH pathophysiology. Several circulating biomarkers of the disease have been identified recently (36). Besides being reflections of the pathological processes in the lung vasculature, the circulating factors can potentially cause dysfunction in other vascular beds. Indeed, dysregulation of the cerebral blood flow in PAH patient has been demonstrated, which was improved by treatment with sildenafil and worsened by iloprost (37). Thus, systemic vasculature can be affected by disease in PAH. Potentially, adaptation mechanisms caused by RV pressure overload can be hampered by the PAH pathologic process affecting coronary circulation.

2. Animal models

Animal models do not fully reflect human diseases and have some limitations due to differences genetics, metabolism, and physiology. Despite these limitations, animal models deliver valuable information physiology, adaptation mechanisms to noxious stimuli (Table 1). Genetically modified organisms (e.g. mice) deliver a unique opportunity to investigate genetics and molecular mechanisms of human diseases. In PAH field of research, several models have been developed potentially reflecting different etiologies (6).

Table 1. Summary of animal models of pulmonary arterial hypertension and right ventricular pressure overload.

Most commonly used models	Rarely used models
Hypoxia exposure • Mice • Rats Monocrotaline injection • •Rats Su5416 + Hypoxia model • Rats Pulmonary artery banding • Mice • Rats	Monocrotaline injection + pneumectomy model Su5416 + pneumectomy model Brisket disease Schistosomiasis associated pulmonary hypertension

Table 2. Overview of the publications with functional characterization of the hypoxia model

Paper	Vascular resistance	Vascular compliance	Cardiac output/index	RV systolic function	RV diastolic function	RV/PA coupling	notes
Crnkovic S et al. Am J Physiol Lung Cell Mol Physiol. 2016 Jul 1;311(1):L59-73	RVSP ↑	n.a.	n.a.	TAPSE ↓ Contractility index ↔	EDP ↔, RV EDD ↑	n.a.	Compensated RV dysfunction
Chai S et al. Transl Res. 2015 Dec;166(6):772-82	RVSP ↑	n.a.	n.a.	n.a.	n.a.	n.a.	Lectin KO mice develop less vascular remodeling in HOX 26470682
Dromparis P et al. Circ Res. 2013 Jul 5;113(2):126-36	mPAP↑	n.a.	n.a.	n.a.	n.a.	n.a.	Normoxic UCP2 KO mice demonstrate HOX phenotype
Hara Y et al. J Clin Invest. 2011 Jul;121(7):2888-97	RVSP ↑	n.a.	n.a.	n.a.	n.a.	n.a.	Multidrug resistance–associated protein 4 is involved in hypoxic PAH development
Ooi CY et al. Am J Physiol Heart Circ Physiol. 2010 Dec;299(6):H1823-31 (NC Chesler group)	mPAP ↑	Elastic modulus ↑	n.a.	n.a.	n.a.	n.a.	Elevated collagen contributes to extralobar PA stiffening in chronic hypoxia
Wang Z et al. J Appl Physiol (1985). 2017 Feb 1;122(2):253-263 (NC Chesler group)	mPAP ↑	PA compliance ↓	CO ↔	n.a.	n.a.	↔	PA collagen content contributes to RV pulsatile load
Brown RD et al. Am J Physiol Heart Circ Physiol. 2013 Jan 15;304(2):H269-81	RVSP ↑	n.a.	CO ↔	RV fractional shortening ↔	n.a.	n.a.	MEKK2 regulates RV hypertrophic remodeling

CO – cardiac output, EDP – end-diastolic pressure, mPAP – mean pulmonary arterial pressure, n.a. – not analysed, PA – pulmonary artery, RV – right ventricle,

RV EDD – right ventricular end-diastolic dimension, RVSP – right ventricular systolic pressure, TAPSE – tricuspid annular plane systolic excursion.

2.1. Hypoxia model

2.1.1. General information

Probably, the most widely used animal model of PAH is the chronic exposure to hypoxia. Pubmed search using key words “animal models” and “pulmonary hypertension” and “hypoxia” results in over 600 publications. Hypoxia model is characterized by moderate pulmonary arterial pressure elevation.

Mostly the term of hypoxia model refers to the model of normobaric hypoxia, where hypoxia is generated by diluting ambient air with nitrogen thereby reducing oxygen concentration most frequently to 10% and its partial pressure to 10 kPa in inspired air. Another approach is the hypobaric hypoxia, where the hypoxia is generated in hypobaric chambers by reducing atmospheric pressure thus reducing partial pressure of oxygen to 10 kPa. This corresponds to the altitude level ca. 4500 m (38).

Morphological substrate of the lung vascular resistance elevation is increased thickening of media of arteries 50-200 μm and muscularization of previously non-muscularized small diameter arteries. Moreover, increase collagen content in the pulmonary extralobular arteries has been demonstrated to cause vascular stiffness elevation (39). Consequently, moderate elevation of the vessel resistance results in right ventricular remodeling and hypertrophy.

2.1.2. Morphological characterization

Chronic hypoxic exposure results in adaptive RV remodeling, which is characterized by cardiomyocyte (CMC) hypertrophy and absence of fibrosis (33, 40). Pressure overload leads to activation of pathologic gene expression profile such as downregulation of SERCA, shift from aMHC to bMHC expression and elevated expression of ANP and BNP.

2.1.3. Functional characterization

Elevated vascular resistance leads to increased mPAP (7). However, most frequently RVSP elevation is used as a surrogate parameter for lung vascular resistance (41-43). Moreover,

pulmonary vascular stiffness increases because of vascular remodeling (39). Due to chronic afterload elevation, cardiac output is reduced but right ventricular contractility measured as contractility index (33) or fractional shortening (40) remains unchanged. RV EDP and Tau increase reflecting diastolic impairment (33). These findings suggest that pressure overload generated by vascular remodeling in chronic hypoxia is not enough to cause RV dysfunction.

The RV/PA coupling has been investigated in only one study and found as not changed (44). Possibly, moderate pressure elevation was completely compensated by adaptive changes in RV.

2.1.4. Combination models

Poels et al. tested the hypothesis that combination of hypoxia and low copper diet could cause RV dysfunction based on previous findings of Bogaard et al. (45). However, they found no worsening of RV function in mice exposed to hypoxia and low copper diet (46). Hypoxic exposure combined with the lack of ABCG2 transporter, a non-selective xenobiotic transporter, lead to RV fibrosis development and diastolic dysfunction (47). Potentially, loss of ABCG2 could result in an intracellular accumulation of porphyrins and haeme degradation products and compromise cellular survival under hypoxia (48).

Table 3. Overview of the publications with functional characterization of the monocrotaline model

Paper	Vascular resistance	Vascular compliance	Cardiac output/index	RV systolic function	RV diastolic function	RV/PA coupling	notes
Our unpublished data	RVSP ↑	n.a.	CO ↓	Contractility index ↓	RV EDP ↑	n.a.	
Barman SA et al. Arterioscler Thromb Vasc Biol. 2014 Aug;34(8):1704-15	RVSP ↑	n.a.	CO ↓	n.a.	n.a.	n.a.	NOX4 in PAH Rat strain -not indicated
Paulin R et al. Circ Res. 2015 Jan 2;116(1):56-69	mPAP ↑		CO ↓in decompensation group	TAPSE ↓	RV EDP ↑	n.a.	miR208-Mef2 axis in RV decompensation. SD rats
Hessel MH et al. Am J Physiol Heart Circ Physiol. 2006 Nov;291(5):H2424-30	RVSP ↑	Ea ↓	CO ↓ in decompensation group	Ees ↔	RV EDP ↑, Eed ↔	Ees/Ea↓*	No RV fibrosis Wistar male rats 200 –250 g
Kosanovic D et al. Respir Res. 2011 Jun 23;12:87	RVSP ↑		CO ↓	TAPSE ↓	Data not shown	n.a.	ET-1 inhibitor reduces RV load and fibrosis. SD rats
Okumura K et al. J Mol Med (Berl). 2015 Jun;93(6):663-74	RVSP ↑	n.a.	CO ↓	Ees ↓	RV Tau ↑	n.a.	Carvedilol treatment improves RV fibrosis and function. SD rats
Pullamsetti SS et al. Arterioscler Thromb Vasc Biol. 2012 Jun;32(6):1354-65	RVSP ↑	n.a.	CI ↓	n.a.	n.a.	n.a.	TK inhibitors in PAH. SD rats
Liu F et al. JCI Insight. 2016 Jun 2;1(8)	RVSP ↑	Shear modulus ↑	n.a	TAPSE ↓	n.a	n.a.	Distal vessel stiffening in PAH. SD rats
Mouchaers KT et al. Eur Respir J. 2010 Oct;36(4):800-7	RVSP and mPAP↑	n.a.	CO and SV ↓	TAPSE ↓	RVEDP ↑	n.a.	Fasudil for treatment of PAH. Wistar rats
Brown MB et al. Am J Physiol Regul Integr Comp Physiol. 2017 Feb 1;312(2):R197-R210	RVSP ↑	n.a.	CI ↓	n.a.	n.a.	n.a.	Exercise training in PAH. SD rats

CI – cardiac index, CO – cardiac output, EDP – end-diastolic pressure, Ea - effective arterial elastance, Ees – end systolic elastance, mPAP – mean pulmonary arterial pressure, n.a. – not analysed, RV – right ventricle, RVSP – right ventricular systolic pressure, SV – stroke volume, TAPSE – tricuspid annular plane systolic excursion. * - calculated by me using values provided in the manuscript.

2.2. Monocrotaline model

2.2.1. General information

Another commonly used model is the monocrotaline (MCT) injection model. In this model, a pyrrolizidine alkaloid isolated from *Crotalaria spectabilis* is injected into rats. Interestingly, while in pulmonology this model is widely used model of pulmonary hypertension, in hepatology MCT injection 2-10 mg/kg body weight is used a model of liver injury, a sinusoidal obstruction syndrome (49). One publication reports myocarditis and coronary arteriolar medial thickening in rats three weeks after MCT injection 50 mg/kg s.c. (50). These changes were accompanied by disturbed systolic and diastolic function. The authors suggest a direct cardiotoxic effect of MCT to be responsible for the observed phenotype.

2.2.2. Morphological characterization

Cardiomyocyte hypertrophy and RV fibrosis development were reported in MCT model (51, 52). Potentially, elevated TGF-b (52) and Tenascin C (53) could mediate RV fibrosis. Analysis of RV fibrosis performed by Sirius red staining of RV samples revealed increase in both perivascular and interstitial fibrosis (51). Interestingly, while cardiomyocyte hypertrophy development stopped after reaching a given level, the fibrosis development continued over the week 4-5 post MCT injection and was paralleled by development of signs of RV decompensation (54). Analysis of RV tissue revealed elevated expression of several matricellular proteins (55). The level of RV fibrosis seems to depend on the degree of RV afterload elevation since significant reduction of lung vascular resistance by ET-1 inhibitor reduced RV fibrosis (51).

On the other hand, others described dose-dependent RV hypertrophy development without fibrosis in this model (56). Of note, this group used Wistar rats and therefore, strain related differences could be a potential explanation for the differences in results.

Changes in RV metabolism have been shown in this model, which could be responsible for the dysfunction phenotype (57, 58).

2.2.3. Functional characterization

Overview of the studies provided a functional characterization of the model is provided on the table 3. This model is characterized by elevated afterload due to elevated lung vascular resistance determined as RVSP (59) and mPAP (54). In addition to the resistance changes, vascular stiffness is elevated as well (60). Pulmonary vascular stiffness elevation occurs as early as one-week post monocrotaline injection and is postulated to be due to remodeling of the distal vessels (60). In the study, vascular stiffness elevation was prevented by chronic treprostinil treatment.

MCT dose-dependently causes a decline in RV functional parameters such as stroke volume and end-systolic elastance (56). Echocardiographic evaluation reveals decrease in stroke volume (61) and TAPSE (60). This leads to reduction in cardiac output (62). Diastolic function is disturbed in this model as indicated by elevated RV EDP (54, 61) and Tau (63). Paulin R et al. demonstrated transition of the compensated RV remodeling at the week 3-4 post MCT injection to the RV decompensation at the weeks 5-6 (54). Comparable functional results were described by Hessel MH et al., who analyzed rats in MCT model after injection of either 30 mg/kg or 80 mg/kg body weight (56). Extensive characterization of this model using pressure-volume loop analysis revealed disturbance in both contractile and diastolic functions (63).

Interference with adrenergic system improved RV function and decreased fibrosis without influencing lung vascular resistance (52). Improvement in both systolic and diastolic parameters was observed. Finally, these changes resulted in improved exercise capacity. Analysis of RV tissue revealed reduced fibrosis, activated adrenergic signaling and reduction TGF-b signaling upon carvedilol treatment. These findings suggest important role of the sympatho-adrenal system dysregulation in development of RV dysfunction. These findings are in line with findings on the SU+HOX model (64, 65).

The question of RV/PA uncoupling remains mainly untouched in the MCT model as well. Interestingly, Hessel et al. in their manuscript provide values of both Ees and Ea, but not provide calculated ratio Ees/Ea. Decreased Ees/Ea shown in the table 3 has been calculated based on the values provided in the respective manuscript. Experimenters that have performed such extensive analysis by pressure-volume loops are certainly aware of Ees/Ea ratio. The lack of this ratio in the manuscript could be explained by the authors knowledge of

the limitations of the RV pressure-loop measurements using conductance catheters. The use of pressure-volume loop analysis using conductance catheters was established for the left ventricle (66) and is based on several assumptions, which cannot be applied to RV due to its different position, shape and contraction pattern.

Several studies investigated the effect of exercise training on RV structure and function in the MCT model. Brown MB et al. demonstrated protective effect of both high-intensity interval training and continuous exercise training on the MCT induced vascular remodeling (67). Protective effect on vascular remodeling resulted in reduction of vascular resistance. This effect could be explained by elevated eNOS expression in the lung tissue as detected by western blot analysis. Only high intensity training improved cardiac function and fibrosis in MCT rats. Analysis of cardiac tissue revealed that high-intensity training induced higher level of apelin expression, an anti-apoptotic, and anti-inflammatory mediator in the heart. None of the training modalities influenced significantly levels of RV tissue inflammation and apoptosis in the study. These results are in line with the findings of the study demonstrating that voluntary exercise delays heart failure onset in MCT rats (68). These experimental studies provide solid support to clinical trials demonstrating beneficial effect of the exercise training on pulmonary arterial pressure, exercise capacity and quality of life in PAH patients (69).

Table 4. Overview of the publications with functional characterization of the Sugen5416+Hypoxia model (SU/HOX)

Paper	Vascular resistance	Vascular compliance	Cardiac output/index	RV systolic function	RV diastolic function	RV/PA coupling	notes
Our unpublished data	RVSP ↑	Wave reflection ↑	CO ↓	Contractility index ↓	RV EDP ↑	n.a.	
Alzoubi A et al. Am J Physiol Heart Circ Physiol. 2013 Jun 15;304(12):H1708-18	RVSP 100 mmHg, TPRI ↑	n.a.	CI ↓	TAPSE ↓	RVEDD ↑	n.a.	DHEA treatment restores RV function
Bogaard HJ et al. Circulation. 2009 Nov 17;120(20):1951-60	RVSP up to 80 mmHg	n.a.	CO, CI ↓	TAPSE, SV ↓	RVID ↑	n.a.	Pressure overload does not explain RHF
de Raaf MA et al. Eur Respir J. 2014 Jul;44(1):160-8	RVSP up to 100 mm Hg	n.a.	n.a.	TAPSE ↓	RVEDD ↑	n.a.	Model characterization, vascular remodeling, partially reversible
de Raaf MA et al. Am J Physiol Lung Cell Mol Physiol. 2015 Nov 15;309(10):L1164-73	RVSP up to 70 mmHg, TPR ↑	n.a.	CO ↔	TAPSE, SV, Ees ↔	RVEDD ↑	↔	Serotonin transporter KO rats
Liu A et al. Physiol Rep. 2017 Mar;5(6)	RVSP up to 45 mmHg	SV/RV PP ↓	CO and CI ↔	SV, Ees ↔	RVEDP ↑	↓	Ovariectomized rats. Estrogen protects from RV metabolic remodeling
Liu F et al. JCI Insight. 2016 Jun 2;1(8)	RVSP ↑	Shear modulus ↑	n.a	TAPSE ↓	n.a	n.a.	Distal vessel stiffening in PAH
Oka M et al. Circ Res. 2007 Mar 30;100(6):923-9	RVSP ↑	n.a.	CO ↓	n.a.	n.a.	n.a.	Rho-kinase acute experiment
Savai R et al. Nat Med. 2014 Nov;20(11):1289-300	RVSP, TPR ↑	n.a.	CO, CI ↓	TAPSE ↓	RVID ↑	n.a.	FOXO1 in PAH
Bogaard HJ et al., Am J Respir Crit Care Med. 2010 Sep 1;182(5):652-60	RVSP ↑	n.a.	CO ↓	TAPSE ↓	RVID ↑	n.a.	Carvedilol treatment improved RV function and fibrosis

CI – cardiac index, CO – cardiac output, EDP – end-diastolic pressure, Ea - effective arterial elastance, Ees – end systolic elastance, mPAP – mean pulmonary arterial pressure, n.a. – not analysed, RV – right ventricle, RV – right ventricle, RV EDD – right ventricular end-diastolic dimension, RVSP – right ventricular systolic pressure, SV – stroke volume, TAPSE – tricuspid annular plane systolic excursion, TPR – total pulmonary resistance.

2.3. Sugen5416+Hypoxia model (SU/HOX)

2.3.1. General information

Lung vasculature remodeling in SU/HOX model in rats has been reported to resemble pathologic features of human disease such as presence of plexiform lesions and neointima formation (70). Thus, this model results in more pronounced vascular resistance changes leading to more pressure overload. Additionally, lung vascular stiffness increase has been reported in this model (60). Since the model has been introduced as a model of severe vascular abnormalities, most of the studies concentrated on characterizing lung vascular remodeling with only a few of published studies so far analyzed RV changes. de Raaf et al. described the model in rats as a model of severe pulmonary hypertension with RVSP elevation up to 100mmHg, which partially reversible (71). Variable sensitivity of different rat strains to this model has been reported (72).

Several attempts to generate a mouse SU/HOX model of PAH failed to generate severe and stable PAH. Analysis of this model in mice using C57BL/6J strain revealed moderate (up to 45 mm Hg) and transient RVSP elevation, which was accompanied by transient RV hypertrophy (73).

2.3.2. Morphological changes

Applying hypoxia together with Sugen 5416 leads to severe pulmonary hypertension development (71) resulting in RV remodeling, which consists of RV hypertrophy and fibrosis accompanied by capillary rarefication and fetal gene program re-activation (74) (Figure 1). Liu et al. described mitochondrial abnormalities in RV of rats in SU/HOX model (75), which is consistent with findings of others (65).

2.3.3. Functional characterization

Overview of the studies provided a functional characterization of the model is provided on the table 4. de Raaf MA reported significant lung vascular resistance elevation in this model, reflected by elevated RVSP and TPR (76). In this study, RVSP was increases up to 100 mmHg

to the end of hypoxic exposure and decreased ~70 mmHg at the end of normoxic observation time. These findings were confirmed by others (77). Another consistent finding was decrease in TAPSE and cardiac output reported in several studies (table 4). Disturbances in either systolic or diastolic function could be responsible for the decrease in cardiac output. All studies performing echocardiography consistently report dilated right ventricle. Unfortunately, diastolic parameters were not assessed in any of the reviewed studies. Thus, the question about mechanism of the decreased cardiac output, systolic or diastolic dysfunction, remains open.

Most of the studies do not address RV/PA coupling in this model, probably, due to technical difficulties in assessing it. de Raaf MA et al. reported no significant change in coupling (76). They reported Ea elevation accompanied by comparable degree of Ees elevation resulting in unchanged RV/PA coupling. Of note, RVSP elevation in this study was 60-70 mmHg. In contrast, Liu A et al. demonstrated a decreased RV/PA coupling (75). Using ovariectomized rat in combination with the Su/HOX model induced an end-systolic pulmonary pressure elevation up to 45-50 mmHg. This lead to doubling of Ea with no substantial changes in Ees resulting in decreased RV/PA coupling. Estrogen treatment improved mitochondrial function leading to Ees elevation and improved coupling. Unfortunately, there was no control group consisting of non-operated rats subjected Su/HOX, therefore the question of RV/PA coupling remains open.

Table 5. Overview of the publications with functional characterization of the pulmonary artery banding model

Paper	Vascular resistance/ Load	Cardiac output/index	RV systolic function	RV diastolic function	RV/PA coupling	notes
Egemnazarov B et al. J Am Soc Echocardiogr. 2015 Jul;28(7):828-43	RVSP ↑	CO ↓	Contractility index ↓	RV EDP ↑	n.a.	PAB causes compensated systolic and diastolic dysfunction
Luitel H et al. Physiol Rep. 2017 Mar;5(6). pii: e13146	RVSP ↑	CO ↓	RV EF ↓	Tau and RV EDP ↑	n.a.	Time course of RV remodeling after PAB
Urashima T et al. Am J Physiol Heart Circ Physiol. 2008 Sep;295(3):H1351-H1368	Gradual ↑ RVSP	CO ↓ in severe group	RV EF ↓ in moderate and severe groups	RV EDP ↑ in severe group	n.a.	Heart failure phenotype in severe constriction PAB group FVB mice
Rain S et al. Circ Heart Fail. 2016 Jul;9(7)	RVSP ↑	CO ↓	SV ↓	RV EDV ↑, Myocardial stiffness ↑	n.a.	Stiffness is elevated due to fibrosis and myofibril stiffness
Bogaard HJ et al. Circulation. 2009 Nov 17;120(20):1951-60	RVSP ↑	CO ↓	SV ↓	RV EDV ↑	n.a.	Pressure overload per se does not cause heart failure
West JD et al. Pulm Circ. 2016 Jun;6(2):211-23	RVSP ↑ mean 40 mm Hg	CO ↔		E/A ↔		CPI211 (antagonist of TPα/TPβ25) treatment reduced RV fibrosis
Hemnes AR et al. Pulm Circ. 2012 Jul;2(3):352-8	RVSP ↑ mean 40 mm Hg	CO ↔	Contractility index ↔	RV EDP ↑	n.a.	Testosterone increases CMC size and enhances fibrosis
Kojonazarov B et al. Pulm Circ. 2013 Dec;3(4):926-35	RVSP ↑	CI ↓	RV MPI ↑ (global function parameter)		n.a.	PPARβ/δ agonist GW0742 reduces RV fibrosis and ↑ function
Mendes-Ferreira P et al. Am J Physiol Heart Circ Physiol. 2016 Jul 1;311(1):H85-95	RVSP ↑ Moderate 50 mm Hg Severe 80 mm Hg	CO ↓ in severe group	EF ↓ in severe group	RV EDP ↑ in severe group	n.a.	Functional changes in severe constriction group Wistar rats

CI – cardiac index, CO – cardiac output, E/A – ratio of the early to late flow peaks determined by doppler EchoCG on tricuspid annulus, EDP – end-diastolic pressure, EF -ejection fraction, n.a. – not analysed, RV – right ventricle, RV – right ventricle, RV EDD – right ventricular end-diastolic dimension, RVSP – right ventricular systolic pressure, SV – stroke volume.

2.4. Pulmonary artery banding model (PAB)

2.4.1. General information

In all previously described models RV changes occur secondary to lung vascular remodeling. Therefore, all interventions targeting lung vasculature cause consequently changes in RV function. To overcome this problem and to be able to investigate the mechanisms of RV remodeling and dysfunction, the model of pulmonary artery banding (PAB) has been developed, where a fixed degree of PA stenosis is generated creating a stable and reproducible degree of afterload elevation (78) (Fig. 4). Nevertheless, the model is criticized as well. The major critic points are: 1) operation introducing changes related to the quality of intervention and post-operative care; 2) sudden afterload elevation resembling rather acute thromboembolism and PAH with its progressive overload elevation.

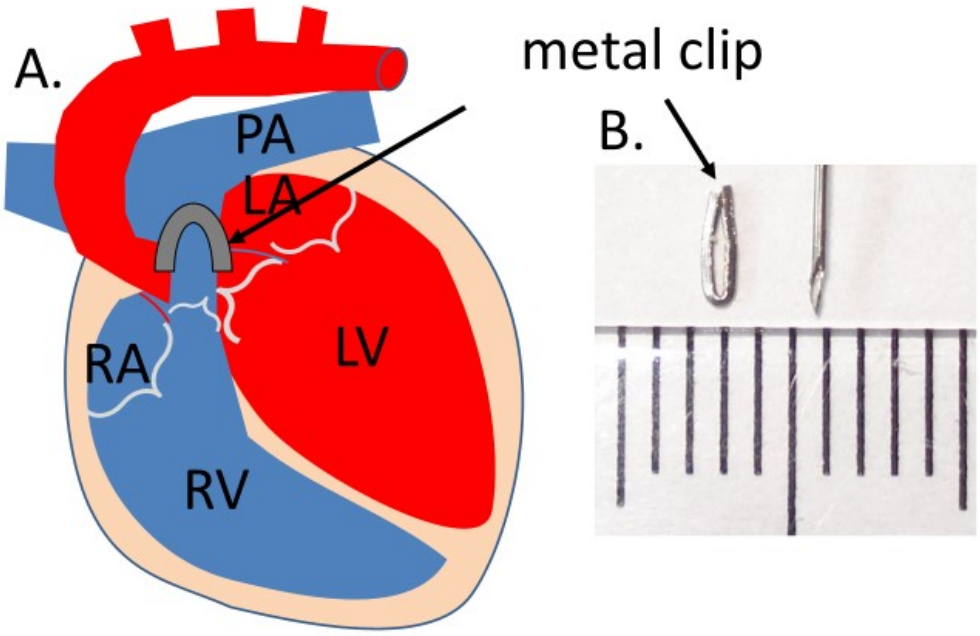

Fig. 4. Schematic representation of the pulmonary artery banding operation. A. The scheme of the heart with demonstration of the placement of the clip on the main pulmonary artery. B. The metal clip constricted to the 0.35 mm is demonstrated next to the scalebar. For

comparison the tip of the 28 G needle is placed next to the clip. Major ticks of the scalebar represent 0.5 cm, minor ticks – 1 mm.

2.4.2. Morphological changes

Pulmonary artery banding (PAB) enables generation of very high afterload elevation, consequently resulting in massive RV hypertrophy and fibrosis (34, 79) (Figure 1). The elevated ventricular expression of TGFβ and collagens 1a1/3a1 (30, 34) along with the increased level of collagen crosslinking molecules (LOX) suggests that not only the amount but also the quality of fibrotic tissue might be affected in this model (80). The degree of RV fibrosis development is dependent on the level of pressure overload (81). In the double hit model of copper-depleted diet and PAB, Bogaard et al. showed increased RV fibrosis by staining and RV dilation as well as capillary rarefaction (45).

2.4.3. Functional characterization

The advantage of the model is the possibility to vary the degree of PA stenosis and generation different degrees of pressure overload which results in gradual pressure elevation (80, 82).

Moderate pressure elevation up to 40 mm Hg does not lead to cardiac output decrease (83, 84). Higher levels of pressure overload are associated with cardiac output decrease (30, 34). In accordance with these findings, a decrease in parameters of contractile function was reported such as contractility index (34), right ventricular ejection fraction (30) and stroke volume (45). Nevertheless, mice or rats after PAB do not demonstrate signs of heart failure (34, 84). In the screened literature, only one publication by Urashima T et al. reports signs such as peripheral edema and liver enlargement in experimental mice group of severe stenosis (80). In contrast to other groups, the authors used FVB mice. Thus, one could speculate that genetic differences between strains could be responsible for the observed phenotype. The straight forward approach would be to compare in one study several mouse strains including FVB and C57Bl/6 mice. Unfortunately, since 2008, the year of publication of the paper by Urashima et al., no other publications appeared from the group using FVB mice in PAB model.

RV diastolic function is disturbed in PAB, which reflected by increased RV EDV, elevated RV EDP and prolonged Tau (30, 34, 81, 82). West JD et al. reported no changes in diastolic parameters despite presence of morphologic signs of RV remodeling such as cardiomyocyte hypertrophy and RV fibrosis (83). However, pressure elevation achieved in the study was around 40 mm Hg, which is rather moderate elevation. This observation suggests that the morphologic substrate of the RV diastolic disfunction in the setting of pressure overload is some other factor but not fibrosis.

Thus, pressure elevation alone does not lead to the RV maladaptation and failure and other stimuli interfering with the adaptation mechanisms are necessary to drive RV towards to failure (45). In their study Bogaard et al. showed that addition of a copper-depleted diet to PAB in rats led to increased RV fibrosis and RV dilation as well as capillary rarefaction. According to their hypothesis, low-copper diet interferes with HIF-1α protein stabilization, which is necessary for VEGF signaling, and therefore subsequently affects angiogenesis (45). Indeed, this model is a model of compensated RV dysfunction (74).

2.5. Transgenic models

Currently, several transgenic models of PAH have been described in literature (85). In these models, genetic defect alone or in combination with another noxious stimulus causes PAH development. Again, a comprehensive analysis of RV structural changes and function is missing, since the investigations were primarily focused on characterization and understanding mechanisms of vascular remodeling.

Overexpression of the AP-1 family member Fra-2, has been reported to cause cardiac fibrosis development (86). The functional consequence of this phenotype is not known yet. The receptor Fn14 and its ligand TWEAK have been associated with the progressive dilated cardiomyopathy and heart failure affecting both the LV and RV (87). In PAB model, Fn-14 KO mice develop less RV fibrosis and dysfunction potentially indicating the involvement of FN-14/RhoA/MRTF signaling pathway in pathogenesis of RV fibrosis (88).

2.6. Rarely used models

2.6.1. Monocrotaline injection + pneumectomy

Monocrotaline model of PAH results in significant pressure elevation and resembles majority of the clinical features of PAH. Morphologically it is characterized by pronounces hypertrophy of the medial layer of the vasculature and muscularization of the previously non-muscularized small caliber arterioles (89). Nevertheless, the model is criticized due to the lack of visual endothelial layer changes such as neointima formation or absence of plexiform lesions. It has been postulated that the addition of the high shear stress to the remodeled vessels would cause endothelial injury and neointima formation. The model has been reported combining MCT injection with the systemic-to-pulmonary circulation shunt (90) and MCT injection combining with the pneumonectomy (91). Both models caused development of neointima formation, whereas the combination of MCT with pneumonectomy caused highest mPAP elevation. Moreover, the model was associated with higher mortality in rats (92). The model has been used to investigate molecular mechanisms of vascular remodeling (93). Since the model was established with the specific aim to generate endothelial changes, RV structural and functional disturbances have not been investigated yet. High mortality and severe level of stress experienced by animals in the model make the use of the combined MCT + pneumonectomy model very challenging.

2.6.2. Su5416 + pneumectomy model

Marked strain specific differences in have been observed in pulmonary hypertension development in SU/HOX model (72). Moreover, SU/HOX model has been shown to induce partially reversible pulmonary hypertension upon return to normoxia despite presence of intimal disturbances (71). The authors postulated that hypoxic signaling is not sufficient to cause persistent vascular remodeling. The authors combined a noxious stimulus Su5416 with the shear stress after pneumectomy to induce severe pulmonary hypertension (94). Su5416 + pneumectomy model (SU/Pnx) has demonstrated progressive RVSP elevation, but after six weeks (at the end of observation period) both SU/HOX and SU/Pnx models showed comparable degree of pressure elevation and cardiac function disturbances. Morphologic analysis revealed comparable degree of media and intima thickening (94). Thus, SU/Pnx

demonstrates progressive RVSP elevation and might be useful for investigations of specific questions related to effects of shear stress on pulmonary vascular intima.

2.6.3. Brisket disease

Brisket disease, a chronic mountain sickness in cattle, is characterized by pulmonary hypertension, right heart enlargement and peripheral edema development (95). It has been described in some sensitive cattle exposed to high altitude (96, 97). Single nucleotide polymorphism analysis in sensitive animals revealed several its association with several genes (98). Due to its similarities to the chronic mountain sickness in humans (99) and its clear association with the hypoxic exposure, the disease can be considered as a model of hypoxic pulmonary hypertension.

2.6.4. Schistosomiasis associated pulmonary hypertension

Schistosomiasis is a parasitic infection caused by the trematode worms of the genus Schistosoma (100). Studies using different approach for detecting pulmonary hypertension in patients with hepatosplenic form of the schistosomiasis report prevalence of PAH ranging between 7.7% and 30% depending on the detection technique (101-103). Based on these observations, an animal model of the disease was developed by infecting mice with the cercariae of the pathogen (104, 105). PAH development was observed in the model, which correlated with the lung egg burden and the levels of inflammatory cytokines (106). Thus, the model might represent some aspects of PAH related to inflammation.

3. Summary

PAH remains a severe disease with poor prognosis. Intensive research is focused on investigating pathomechanisms of pulmonary vascular dysfunction and remodeling (107). Since right ventricular failure is the leading cause of mortality in PAH, an important component of treatment should be the interference with the mechanisms mediating RV failure.

Currently, the research in PAH is focused on revealing mechanisms of pulmonary vascular remodeling and therapeutically targeting it. Research on the right ventricle in PAH seems to be constant and deliver ~10 % of publications in the field. RV has been suggested to the therapeutic target in PAH (108, 109). Nevertheless, the researchers in the field should be sensitized about the topic of RV failure to intensify investigations and development of novel therapies addressing the RV.

The research on the right heart focuses mainly on mechanisms regulating the contractile function of the ventricle. The research on the RV diastolic dysfunction is currently at the level of characterizing it. Our data suggest that both fibrotic changes in the extracellular matrix and disturbances in calcium handling mechanisms could contribute to diastolic dysfunction in PAH, which is in line with the observations of others (28). PAB, MCT and SU/HOX models of PAH are characterized by pronounced RV fibrosis development. Reduction of RV fibrosis has been shown upon treatment with vasodilating agents in hypoxia and MCT models. Since the observed reduction in fibrosis could be the consequence of either hemodynamic unloading or direct effects on the heart, the interpretation of the obtained results is difficult. Our unpublished data suggest that anti-fibrotic therapy does not lead to functional improvement.

RV/PA coupling is rarely analyzed in small animal studies, perhaps due to technical difficulties. Mostly, RV/PA coupling is calculated from the pressure-loop measurements performed using conductance catheters inserted into RV. However, electric conductance-based measurements of ventricular volume have been established for LV with its cylindric form. The assumptions behind this measurement do not work in the case of RV with its complex form. Moreover, systole-diastolic changes in of LV volumes are radial, while RV volume changes are mostly due to longitudinal movement. Thus, even if one attempts to determine only difference between systole and diastole, the method delivers questionable results. This might explain our finding that this parameter is rarely determined in experimental studies.

Potentially, RV/PA coupling could deliver important information about adaptation mechanisms to pressure overload. Impairment of RV/PA coupling has been reported in PAH patients and in animal models of RV pressure overload. It is determined as ventricular contractility increased adequately to load elevation. The question remains open whether this is an adaptive mechanism or sign of maladaptation.

Genetic factors contributing to the development of RV failure remain poorly understood. Genetic markers of RV failure signature were published (74). However, these findings require confirmation and testing on patient cohorts. A promising approach is the investigations of genetically modified animals (mice and rats) in the established models of RV pressure overload. Cardiac fibrosis was reported in the Fra-2 overexpressing mice (86). However, the functional consequence of the observed phenotype is unclear. More sophisticated approach combining molecular analysis with functional characterization revealed involvement of FN-14/RhoA/MRTF signaling in development of RV fibrosis (88). Currently, majority of the generated transgenic animals have not been characterized in terms of RV structure and function.

In summary, currently investigations on the mechanisms of the RV failure on animal models are at the level of characterizing it. There are no models completely resembling all clinical features of the human disease. The question of the RV/PA uncoupling remains mainly untouched topic. Molecular mechanisms of RV dysfunction and failure seem to have some specific features compared to LV.

Literature

1. Galie N, Hoeper MM, Humbert M, Torbicki A, Vachiery JL, Barbera JA, et al. Guidelines for the diagnosis and treatment of pulmonary hypertension: the Task Force for the Diagnosis and Treatment of Pulmonary Hypertension of the European Society of Cardiology (ESC) and the European Respiratory Society (ERS), endorsed by the International Society of Heart and Lung Transplantation (ISHLT). European heart journal. 2009;30(20):2493-537.
2. Voelkel NF, Gomez-Arroyo J, Abbate A, Bogaard HJ. Mechanisms of right heart failure-A work in progress and a plea for failure prevention. Pulmonary circulation. 2013;3(1):137-43.
3. Wang GY, McCloskey DT, Turcato S, Swigart PM, Simpson PC, Baker AJ. Contrasting inotropic responses to alpha1-adrenergic receptor stimulation in left versus right ventricular myocardium. American journal of physiology Heart and circulatory physiology. 2006;291(4):H2013-7.
4. Irlbeck M, Muhling O, Iwai T, Zimmer HG. Different response of the rat left and right heart to norepinephrine. Cardiovascular research. 1996;31(1):157-62.
5. Modesti PA, Vanni S, Bertolozzi I, Cecioni I, Lumachi C, Perna AM, et al. Different growth factor activation in the right and left ventricles in experimental volume overload. Hypertension. 2004;43(1):101-8.
6. Colvin KL, Yeager ME. Animal Models of Pulmonary Hypertension: Matching Disease Mechanisms to Etiology of the Human Disease. Journal of pulmonary & respiratory medicine. 2014;4(4).
7. Dromparis P, Paulin R, Sutendra G, Qi AC, Bonnet S, Michelakis ED. Uncoupling protein 2 deficiency mimics the effects of hypoxia and endoplasmic reticulum stress on mitochondria and triggers pseudohypoxic pulmonary vascular remodeling and pulmonary hypertension. Circulation research. 2013;113(2):126-36.
8. Lankhaar JW, Westerhof N, Faes TJ, Gan CT, Marques KM, Boonstra A, et al. Pulmonary vascular resistance and compliance stay inversely related during treatment of pulmonary hypertension. European heart journal. 2008;29(13):1688-95.
9. Saouti N, Westerhof N, Helderman F, Marcus JT, Boonstra A, Postmus PE, et al. Right ventricular oscillatory power is a constant fraction of total power irrespective of pulmonary artery pressure. American journal of respiratory and critical care medicine. 2010;182(10):1315-20.
10. Mahapatra S, Nishimura RA, Sorajja P, Cha S, McGoon MD. Relationship of pulmonary arterial capacitance and mortality in idiopathic pulmonary arterial hypertension. Journal of the American College of Cardiology. 2006;47(4):799-803.
11. Gan CT, Lankhaar JW, Westerhof N, Marcus JT, Becker A, Twisk JW, et al. Noninvasively assessed pulmonary artery stiffness predicts mortality in pulmonary arterial hypertension. Chest. 2007;132(6):1906-12.
12. Liu Z, Brin KP, Yin FC. Estimation of total arterial compliance: an improved method and evaluation of current methods. The American journal of physiology. 1986;251(3 Pt 2):H588-600.
13. Stergiopulos N, Meister JJ, Westerhof N. Simple and accurate way for estimating total and segmental arterial compliance: the pulse pressure method. Annals of biomedical engineering. 1994;22(4):392-7.
14. Randall OS, van den Bos GC, Westerhof N. Systemic compliance: does it play a role in the genesis of essential hypertension? Cardiovascular research. 1984;18(8):455-62.
15. Abraham DM, Davis RT, 3rd, Warren CM, Mao L, Wolska BM, Solaro RJ, et al. beta-Arrestin mediates the Frank-Starling mechanism of cardiac contractility. Proceedings of the National Academy of Sciences of the United States of America. 2016;113(50):14426-31.
16. Monroe RG, Gamble WJ, LaFarge CG, Kumar AE, Stark J, Sanders GL, et al. The Anrep effect reconsidered. The Journal of clinical investigation. 1972;51(10):2573-83.

17. Mohl MC, Iismaa SE, Xiao XH, Friedrich O, Wagner S, Nikolova-Krstevski V, et al. Regulation of murine cardiac contractility by activation of alpha(1A)-adrenergic receptor-operated Ca(2+) entry. Cardiovascular research. 2011;91(2):310-9.
18. Drawnel FM, Archer CR, Roderick HL. The role of the paracrine/autocrine mediator endothelin-1 in regulation of cardiac contractility and growth. British journal of pharmacology. 2013;168(2):296-317.
19. Cingolani OH, Kass DA. Pressure-volume relation analysis of mouse ventricular function. American journal of physiology Heart and circulatory physiology. 2011;301(6):H2198-206.
20. Brimioulle S, Wauthy P, Ewalenko P, Rondelet B, Vermeulen F, Kerbaul F, et al. Single-beat estimation of right ventricular end-systolic pressure-volume relationship. American journal of physiology Heart and circulatory physiology. 2003;284(5):H1625-30.
21. de Man FS, Handoko ML, van Ballegoij JJ, Schalij I, Bogaards SJ, Postmus PE, et al. Bisoprolol delays progression towards right heart failure in experimental pulmonary hypertension. Circulation Heart failure. 2012;5(1):97-105.
22. Sagawa K. Cardiac contraction and the pressure-volume relationship. New York: Oxford University Press; 1988.
23. Tedford RJ, Mudd JO, Girgis RE, Mathai SC, Zaiman AL, Housten-Harris T, et al. Right ventricular dysfunction in systemic sclerosis-associated pulmonary arterial hypertension. Circulation Heart failure. 2013;6(5):953-63.
24. Kuehne T, Yilmaz S, Steendijk P, Moore P, Groenink M, Saaed M, et al. Magnetic resonance imaging analysis of right ventricular pressure-volume loops: in vivo validation and clinical application in patients with pulmonary hypertension. Circulation. 2004;110(14):2010-6.
25. F. VN, Dietmar S. The Right Ventricle in Health and Disease: Humana Press; 2015.
26. Vonk Noordegraaf A, Galie N. The role of the right ventricle in pulmonary arterial hypertension. European respiratory review : an official journal of the European Respiratory Society. 2011;20(122):243-53.
27. Bogaard HJ, Abe K, Vonk Noordegraaf A, Voelkel NF. The right ventricle under pressure: cellular and molecular mechanisms of right-heart failure in pulmonary hypertension. Chest. 2009;135(3):794-804.
28. Rain S, Handoko ML, Trip P, Gan CT, Westerhof N, Stienen GJ, et al. Right ventricular diastolic impairment in patients with pulmonary arterial hypertension. Circulation. 2013;128(18):2016-25, 1-10.
29. Tanaka Y, Takase B, Yao T, Ishihara M. Right ventricular electrical remodeling and arrhythmogenic substrate in rat pulmonary hypertension. American journal of respiratory cell and molecular biology. 2013;49(3):426-36.
30. Luitel H, Sydykov A, Schymura Y, Mamazhakypov A, Janssen W, Pradhan K, et al. Pressure overload leads to an increased accumulation and activity of mast cells in the right ventricle. Physiological reports. 2017;5(6).
31. Matthews JC, McLaughlin V. Acute right ventricular failure in the setting of acute pulmonary embolism or chronic pulmonary hypertension: a detailed review of the pathophysiology, diagnosis, and management. Current cardiology reviews. 2008;4(1):49-59.
32. Buser M, Felizeter-Kessler M, Lenggenhager D, Maeder MT. Rapidly progressive pulmonary hypertension in a patient with pulmonary tumor thrombotic microangiopathy. American journal of respiratory and critical care medicine. 2015;191(6):711-2.
33. Crnkovic S, Schmidt A, Egemnazarov B, Wilhelm J, Marsh LM, Ghanim B, et al. Functional and molecular factors associated with TAPSE in hypoxic pulmonary hypertension. American journal of physiology Lung cellular and molecular physiology. 2016;311(1):L59-73.
34. Egemnazarov B, Schmidt A, Crnkovic S, Sydykov A, Nagy BM, Kovacs G, et al. Pressure Overload Creates Right Ventricular Diastolic Dysfunction in a Mouse Model: Assessment by Echocardiography. Journal of the American Society of Echocardiography : official publication of the American Society of Echocardiography. 2015;28(7):828-43.

35. Zhang DY, Anderson AS. The sympathetic nervous system and heart failure. Cardiology clinics. 2014;32(1):33-45, vii.
36. Foris V, Kovacs G, Tscherner M, Olschewski A, Olschewski H. Biomarkers in pulmonary hypertension: what do we know? Chest. 2013;144(1):274-83.
37. Rosengarten B, Schermuly RT, Voswinckel R, Kohstall MG, Olschewski H, Weissmann N, et al. Sildenafil improves dynamic vascular function in the brain: studies in patients with pulmonary hypertension. Cerebrovascular diseases. 2006;21(3):194-200.
38. Peacock AJ. ABC of oxygen: oxygen at high altitude. Bmj. 1998;317(7165):1063-6.
39. Ooi CY, Wang Z, Tabima DM, Eickhoff JC, Chesler NC. The role of collagen in extralobar pulmonary artery stiffening in response to hypoxia-induced pulmonary hypertension. American journal of physiology Heart and circulatory physiology. 2010;299(6):H1823-31.
40. Brown RD, Ambler SK, Li M, Sullivan TM, Henry LN, Crossno JT, Jr., et al. MAP kinase kinase kinase-2 (MEKK2) regulates hypertrophic remodeling of the right ventricle in hypoxia-induced pulmonary hypertension. American journal of physiology Heart and circulatory physiology. 2013;304(2):H269-81.
41. Chai S, Wang W, Liu J, Guo H, Zhang Z, Wang C, et al. Leptin knockout attenuates hypoxia-induced pulmonary arterial hypertension by inhibiting proliferation of pulmonary arterial smooth muscle cells. Translational research : the journal of laboratory and clinical medicine. 2015;166(6):772-82.
42. Lang M, Kojonazarov B, Tian X, Kalymbetov A, Weissmann N, Grimminger F, et al. The soluble guanylate cyclase stimulator riociguat ameliorates pulmonary hypertension induced by hypoxia and SU5416 in rats. PloS one. 2012;7(8):e43433.
43. Hara Y, Sassi Y, Guibert C, Gambaryan N, Dorfmuller P, Eddahibi S, et al. Inhibition of MRP4 prevents and reverses pulmonary hypertension in mice. The Journal of clinical investigation. 2011;121(7):2888-97.
44. Wang Z, Schreier DA, Abid H, Hacker TA, Chesler NC. Pulmonary vascular collagen content, not cross-linking, contributes to right ventricular pulsatile afterload and overload in early pulmonary hypertension. Journal of applied physiology. 2017;122(2):253-63.
45. Bogaard HJ, Natarajan R, Henderson SC, Long CS, Kraskauskas D, Smithson L, et al. Chronic pulmonary artery pressure elevation is insufficient to explain right heart failure. Circulation. 2009;120(20):1951-60.
46. Poels EM, Bitsch N, Slenter JM, Kooi ME, de Theije CC, de Windt LJ, et al. Supplementing exposure to hypoxia with a copper depleted diet does not exacerbate right ventricular remodeling in mice. PloS one. 2014;9(4):e92983.
47. Nagy BM, Nagaraj C, Egemnazarov B, Kwapiszewska G, Stauber RE, Avian A, et al. Lack of ABCG2 Leads to Biventricular Dysfunction and Remodeling in Response to Hypoxia. Frontiers in physiology. 2017;8:98.
48. Krishnamurthy P, Ross DD, Nakanishi T, Bailey-Dell K, Zhou S, Mercer KE, et al. The stem cell marker Bcrp/ABCG2 enhances hypoxic cell survival through interactions with heme. The Journal of biological chemistry. 2004;279(23):24218-25.
49. Conotte R, Colet JM. A metabonomic evaluation of the monocrotaline-induced sinusoidal obstruction syndrome (SOS) in rats. Toxicology and applied pharmacology. 2014;276(2):147-56.
50. Akhavein F, St-Michel EJ, Seifert E, Rohlicek CV. Decreased left ventricular function, myocarditis, and coronary arteriolar medial thickening following monocrotaline administration in adult rats. Journal of applied physiology. 2007;103(1):287-95.
51. Kosanovic D, Kojonazarov B, Luitel H, Dahal BK, Sydykov A, Cornitescu T, et al. Therapeutic efficacy of TBC3711 in monocrotaline-induced pulmonary hypertension. Respiratory research. 2011;12:87.
52. Okumura K, Kato H, Honjo O, Breitling S, Kuebler WM, Sun M, et al. Carvedilol improves biventricular fibrosis and function in experimental pulmonary hypertension. Journal of molecular medicine. 2015;93(6):663-74.

53. Hessel M, Steendijk P, den Adel B, Schutte C, van der Laarse A. Pressure overload-induced right ventricular failure is associated with re-expression of myocardial tenascin-C and elevated plasma tenascin-C levels. Cellular physiology and biochemistry : international journal of experimental cellular physiology, biochemistry, and pharmacology. 2009;24(3-4):201-10.
54. Paulin R, Sutendra G, Gurtu V, Dromparis P, Haromy A, Provencher S, et al. A miR-208-Mef2 axis drives the decompensation of right ventricular function in pulmonary hypertension. Circulation research. 2015;116(1):56-69.
55. Imoto K, Okada M, Yamawaki H. Expression profile of matricellular proteins in hypertrophied right ventricle of monocrotaline-induced pulmonary hypertensive rats. The Journal of veterinary medical science. 2017;79(6):1096-102.
56. Hessel MH, Steendijk P, den Adel B, Schutte CI, van der Laarse A. Characterization of right ventricular function after monocrotaline-induced pulmonary hypertension in the intact rat. American journal of physiology Heart and circulatory physiology. 2006;291(5):H2424-30.
57. Nagendran J, Gurtu V, Fu DZ, Dyck JR, Haromy A, Ross DB, et al. A dynamic and chamber-specific mitochondrial remodeling in right ventricular hypertrophy can be therapeutically targeted. The Journal of thoracic and cardiovascular surgery. 2008;136(1):168-78, 78 e1-3.
58. Piao L, Fang YH, Cadete VJ, Wietholt C, Urboniene D, Toth PT, et al. The inhibition of pyruvate dehydrogenase kinase improves impaired cardiac function and electrical remodeling in two models of right ventricular hypertrophy: resuscitating the hibernating right ventricle. Journal of molecular medicine. 2010;88(1):47-60.
59. Barman SA, Chen F, Su Y, Dimitropoulou C, Wang Y, Catravas JD, et al. NADPH oxidase 4 is expressed in pulmonary artery adventitia and contributes to hypertensive vascular remodeling. Arteriosclerosis, thrombosis, and vascular biology. 2014;34(8):1704-15.
60. Liu F, Haeger CM, Dieffenbach PB, Sicard D, Chrobak I, Coronata AM, et al. Distal vessel stiffening is an early and pivotal mechanobiological regulator of vascular remodeling and pulmonary hypertension. JCI insight. 2016;1(8).
61. Mouchaers KT, Schalij I, de Boer MA, Postmus PE, van Hinsbergh VW, van Nieuw Amerongen GP, et al. Fasudil reduces monocrotaline-induced pulmonary arterial hypertension: comparison with bosentan and sildenafil. The European respiratory journal. 2010;36(4):800-7.
62. Pullamsetti SS, Berghausen EM, Dabral S, Tretyn A, Butrous E, Savai R, et al. Role of Src tyrosine kinases in experimental pulmonary hypertension. Arteriosclerosis, thrombosis, and vascular biology. 2012;32(6):1354-65.
63. Alaa M, Abdellatif M, Tavares-Silva M, Oliveira-Pinto J, Lopes L, Leite S, et al. Right ventricular end-diastolic stiffness heralds right ventricular failure in monocrotaline-induced pulmonary hypertension. American journal of physiology Heart and circulatory physiology. 2016;311(4):H1004-H13.
64. Bogaard HJ, Natarajan R, Mizuno S, Abbate A, Chang PJ, Chau VQ, et al. Adrenergic receptor blockade reverses right heart remodeling and dysfunction in pulmonary hypertensive rats. American journal of respiratory and critical care medicine. 2010;182(5):652-60.
65. Drake JI, Gomez-Arroyo J, Dumur CI, Kraskauskas D, Natarajan R, Bogaard HJ, et al. Chronic carvedilol treatment partially reverses the right ventricular failure transcriptional profile in experimental pulmonary hypertension. Physiological genomics. 2013;45(12):449-61.
66. Pacher P, Nagayama T, Mukhopadhyay P, Batkai S, Kass DA. Measurement of cardiac function using pressure-volume conductance catheter technique in mice and rats. Nature protocols. 2008;3(9):1422-34.
67. Brown MB, Neves E, Long G, Graber J, Gladish B, Wiseman A, et al. High-intensity interval training, but not continuous training, reverses right ventricular hypertrophy and dysfunction in a rat model of pulmonary hypertension. American journal of physiology Regulatory, integrative and comparative physiology. 2017;312(2):R197-R210.
68. Natali AJ, Fowler ED, Calaghan SC, White E. Voluntary exercise delays heart failure onset in rats with pulmonary artery hypertension. American journal of physiology Heart and circulatory physiology. 2015;309(3):H421-4.

69. Pandey A, Garg S, Khunger M, Garg S, Kumbhani DJ, Chin KM, et al. Efficacy and Safety of Exercise Training in Chronic Pulmonary Hypertension: Systematic Review and Meta-Analysis. Circulation Heart failure. 2015;8(6):1032-43.
70. Toba M, Alzoubi A, O'Neill KD, Gairhe S, Matsumoto Y, Oshima K, et al. Temporal hemodynamic and histological progression in Sugen5416/hypoxia/normoxia-exposed pulmonary arterial hypertensive rats. American journal of physiology Heart and circulatory physiology. 2014;306(2):H243-50.
71. de Raaf MA, Schalij I, Gomez-Arroyo J, Rol N, Happe C, de Man FS, et al. SuHx rat model: partly reversible pulmonary hypertension and progressive intima obstruction. The European respiratory journal. 2014;44(1):160-8.
72. Jiang B, Deng Y, Suen C, Taha M, Chaudhary KR, Courtman DW, et al. Marked Strain-Specific Differences in the SU5416 Rat Model of Severe Pulmonary Arterial Hypertension. American journal of respiratory cell and molecular biology. 2016;54(4):461-8.
73. Vitali SH, Hansmann G, Rose C, Fernandez-Gonzalez A, Scheid A, Mitsialis SA, et al. The Sugen 5416/hypoxia mouse model of pulmonary hypertension revisited: long-term follow-up. Pulmonary circulation. 2014;4(4):619-29.
74. Drake JI, Bogaard HJ, Mizuno S, Clifton B, Xie B, Gao Y, et al. Molecular signature of a right heart failure program in chronic severe pulmonary hypertension. American journal of respiratory cell and molecular biology. 2011;45(6):1239-47.
75. Liu A, Philip J, Vinnakota KC, Van den Bergh F, Tabima DM, Hacker T, et al. Estrogen maintains mitochondrial content and function in the right ventricle of rats with pulmonary hypertension. Physiological reports. 2017;5(6).
76. de Raaf MA, Kroeze Y, Middelman A, de Man FS, de Jong H, Vonk-Noordegraaf A, et al. Serotonin transporter is not required for the development of severe pulmonary hypertension in the Sugen hypoxia rat model. American journal of physiology Lung cellular and molecular physiology. 2015;309(10):L1164-73.
77. Alzoubi A, Toba M, Abe K, O'Neill KD, Rocic P, Fagan KA, et al. Dehydroepiandrosterone restores right ventricular structure and function in rats with severe pulmonary arterial hypertension. American journal of physiology Heart and circulatory physiology. 2013;304(12):H1708-18.
78. Tarnavski O, McMullen JR, Schinke M, Nie Q, Kong S, Izumo S. Mouse cardiac surgery: comprehensive techniques for the generation of mouse models of human diseases and their application for genomic studies. Physiological genomics. 2004;16(3):349-60.
79. Kojonazarov B, Novoyatleva T, Boehm M, Happe C, Sibinska Z, Tian X, et al. p38 MAPK Inhibition Improves Heart Function in Pressure-Loaded Right Ventricular Hypertrophy. American journal of respiratory cell and molecular biology. 2017;57(5):603-14.
80. Urashima T, Zhao M, Wagner R, Fajardo G, Farahani S, Quertermous T, et al. Molecular and physiological characterization of RV remodeling in a murine model of pulmonary stenosis. American journal of physiology Heart and circulatory physiology. 2008;295(3):H1351-H68.
81. Rain S, Andersen S, Najafi A, Gammelgaard Schultz J, da Silva Goncalves Bos D, Handoko ML, et al. Right Ventricular Myocardial Stiffness in Experimental Pulmonary Arterial Hypertension: Relative Contribution of Fibrosis and Myofibril Stiffness. Circulation Heart failure. 2016;9(7).
82. Mendes-Ferreira P, Santos-Ribeiro D, Adao R, Maia-Rocha C, Mendes-Ferreira M, Sousa-Mendes C, et al. Distinct right ventricle remodeling in response to pressure overload in the rat. American journal of physiology Heart and circulatory physiology. 2016;311(1):H85-95.
83. West JD, Voss BM, Pavliv L, de Caestecker M, Hemnes AR, Carrier EJ. Antagonism of the thromboxane-prostanoid receptor is cardioprotective against right ventricular pressure overload. Pulmonary circulation. 2016;6(2):211-23.
84. Hemnes AR, Maynard KB, Champion HC, Gleaves L, Penner N, West J, et al. Testosterone negatively regulates right ventricular load stress responses in mice. Pulmonary circulation. 2012;2(3):352-8.
85. West J, Hemnes A. Experimental and transgenic models of pulmonary hypertension. Comprehensive Physiology. 2011;1(2):769-82.

86. Venalis P, Kumanovics G, Schulze-Koops H, Distler A, Dees C, Zerr P, et al. Cardiomyopathy in murine models of systemic sclerosis. Arthritis & rheumatology. 2015;67(2):508-16.
87. Jain M, Jakubowski A, Cui L, Shi J, Su L, Bauer M, et al. A novel role for tumor necrosis factor-like weak inducer of apoptosis (TWEAK) in the development of cardiac dysfunction and failure. Circulation. 2009;119(15):2058-68.
88. Novoyatleva T, Schymura Y, Janssen W, Strobl F, Swiercz JM, Patra C, et al. Deletion of Fn14 receptor protects from right heart fibrosis and dysfunction. Basic research in cardiology. 2013;108(2):325.
89. Schermuly RT, Kreisselmeier KP, Ghofrani HA, Samidurai A, Pullamsetti S, Weissmann N, et al. Antiremodeling effects of iloprost and the dual-selective phosphodiesterase 3/4 inhibitor tolafentrine in chronic experimental pulmonary hypertension. Circulation research. 2004;94(8):1101-8.
90. Tanaka Y, Schuster DP, Davis EC, Patterson GA, Botney MD. The role of vascular injury and hemodynamics in rat pulmonary artery remodeling. The Journal of clinical investigation. 1996;98(2):434-42.
91. Okada K, Tanaka Y, Bernstein M, Zhang W, Patterson GA, Botney MD. Pulmonary hemodynamics modify the rat pulmonary artery response to injury. A neointimal model of pulmonary hypertension. The American journal of pathology. 1997;151(4):1019-25.
92. Polonio IB, Acencio MM, Pazetti R, Almeida FM, Canzian M, Silva BS, et al. Comparison of two experimental models of pulmonary hypertension. Jornal brasileiro de pneumologia : publicacao oficial da Sociedade Brasileira de Pneumologia e Tisilogia. 2012;38(4):452-60.
93. Strobl M, Schreiber C, Panzenbock A, Winter MP, Bergmeister H, Jakowitsch J, et al. Exhaled nitric oxide measurement to monitor pulmonary hypertension in a pneumonectomy-monocrotaline rat model. American journal of physiology Lung cellular and molecular physiology. 2013;305(7):L485-90.
94. Happe CM, de Raaf MA, Rol N, Schalij I, Vonk-Noordegraaf A, Westerhof N, et al. Pneumonectomy combined with SU5416 induces severe pulmonary hypertension in rats. American journal of physiology Lung cellular and molecular physiology. 2016;310(11):L1088-97.
95. Puntriano GO. Physiological basis of brisket disease in cattle. Journal of the American Veterinary Medical Association. 1954;125(931):327-9.
96. Weir EK, Tucker A, Reeves JT, Will DH, Grover RF. The genetic factor influencing pulmonary hypertension in cattle at high altitude. Cardiovascular research. 1974;8(6):745-9.
97. Will DH, Hicks JL, Card CS, Alexander AF. Inherited susceptibility of cattle to high-altitude pulmonary hypertension. J Appl Physiol. 1975;38(3):491-4.
98. Newman JH, Holt TN, Hedges LK, Womack B, Memon SS, Willers ED, et al. High-altitude pulmonary hypertension in cattle (brisket disease): Candidate genes and gene expression profiling of peripheral blood mononuclear cells. Pulmonary circulation. 2011;1(4):462-9.
99. Naeije R. Pulmonary circulation at high altitude. Respiration; international review of thoracic diseases. 1997;64(6):429-34.
100. Kolosionek E, Graham BB, Tuder RM, Butrous G. Pulmonary vascular disease associated with parasitic infection--the role of schistosomiasis. Clinical microbiology and infection : the official publication of the European Society of Clinical Microbiology and Infectious Diseases. 2011;17(1):15-24.
101. Lapa M, Dias B, Jardim C, Fernandes CJ, Dourado PM, Figueiredo M, et al. Cardiopulmonary manifestations of hepatosplenic schistosomiasis. Circulation. 2009;119(11):1518-23.
102. Lapa MS, Ferreira EV, Jardim C, Martins Bdo C, Arakaki JS, Souza R. [Clinical characteristics of pulmonary hypertension patients in two reference centers in the city of Sao Paulo]. Revista da Associacao Medica Brasileira. 2006;52(3):139-43.
103. Rocha RL, Pedroso ER, Rocha MO, Lambertucci JR, Greco DB, Ferreira CE. [Chronic pulmonary form of schistosomiasis mansoni. Clinico-radiologic evaluation]. Revista da Sociedade Brasileira de Medicina Tropical. 1990;23(2):83-9.
104. Smithers SR, Terry RJ. The infection of laboratory hosts with cercariae of Schistosoma mansoni and the recovery of the adult worms. Parasitology. 1965;55(4):695-700.

105. Vilar MM, Pinto RM. Reappraisal of experimental infections with cercariae and schistosomula of a Brazilian strain of Schistosoma mansoni in mice. Brazilian journal of biology = Revista brasleira de biologia. 2005;65(4):729-33.
106. Crosby A, Jones FM, Southwood M, Stewart S, Schermuly R, Butrous G, et al. Pulmonary vascular remodeling correlates with lung eggs and cytokines in murine schistosomiasis. American journal of respiratory and critical care medicine. 2010;181(3):279-88.
107. Ghataorhe P, Rhodes CJ, Harbaum L, Attard M, Wharton J, Wilkins MR. Pulmonary arterial hypertension - progress in understanding the disease and prioritizing strategies for drug development. Journal of internal medicine. 2017;282(2):129-41.
108. Gomez-Arroyo J, Sandoval J, Simon MA, Dominguez-Cano E, Voelkel NF, Bogaard HJ. Treatment for pulmonary arterial hypertension-associated right ventricular dysfunction. Annals of the American Thoracic Society. 2014;11(7):1101-15.
109. So PP, Davies RA, Chandy G, Stewart D, Beanlands RS, Haddad H, et al. Usefulness of beta-blocker therapy and outcomes in patients with pulmonary arterial hypertension. The American journal of cardiology. 2012;109(10):1504-9.